



**University of
Zurich^{UZH}**

**Zurich Open Repository and
Archive**

University of Zurich
University Library
Strickhofstrasse 39
CH-8057 Zurich
www.zora.uzh.ch

Year: 2018

Magnetic tweezers optimized to exert high forces over extended distances from the magnet in multicellular systems

Selvaggi, L ; Pasakarnis, L ; Brunner, D ; Aegerter, C M

Abstract: Magnetic tweezers are mainly divided into two classes depending on the ability of applying torque or forces to the magnetic probe. We focused on the second category and designed a device composed by a single electromagnet equipped with a core having a special asymmetric profile to exert forces as large as 230 pN–2.8 m Dynabeads at distances in excess of 100 m from the magnetic tip. Compared to existing solutions our magnetic tweezers overcome important limitations, opening new experimental paths for the study of a wide range of materials in a variety of biophysical research settings. We discuss the benefits and drawbacks of different magnet core characteristics, which led us to design the current core profile. To demonstrate the usefulness of our magnetic tweezers, we determined the microrheological properties inside embryos of *Drosophila melanogaster* during the syncytial stage. Measurements in different locations along the dorsal-ventral axis of the embryos showed little variation, with a slight increase in cytoplasm viscosity at the periphery of the embryos. The mean cytoplasm viscosity we obtain by active force exertion inside the embryos is comparable to that determined passively using high-speed video microrheology.

DOI: <https://doi.org/10.1063/1.5010788>

Posted at the Zurich Open Repository and Archive, University of Zurich

ZORA URL: <https://doi.org/10.5167/uzh-156915>

Journal Article

Published Version

Originally published at:

Selvaggi, L; Pasakarnis, L; Brunner, D; Aegerter, C M (2018). Magnetic tweezers optimized to exert high forces over extended distances from the magnet in multicellular systems. *Review of Scientific Instruments*, 89(4):045106.

DOI: <https://doi.org/10.1063/1.5010788>

Magnetic tweezers optimized to exert high forces over extended distances from the magnet in multicellular systems

L. Selvaggi, L. Pasakarnis, D. Brunner, and C. M. Aegerter

Citation: [Review of Scientific Instruments](#) **89**, 045106 (2018); doi: 10.1063/1.5010788

View online: <https://doi.org/10.1063/1.5010788>

View Table of Contents: <http://aip.scitation.org/toc/rsi/89/4>

Published by the [American Institute of Physics](#)

Articles you may be interested in

[A force calibration standard for magnetic tweezers](#)

[Review of Scientific Instruments](#) **85**, 123114 (2014); 10.1063/1.4904148

[Magnetic tweezers with high permeability electromagnets for fast actuation of magnetic beads](#)

[Review of Scientific Instruments](#) **86**, 044701 (2015); 10.1063/1.4916255

[BaHigh-force magnetic tweezers with force feedback for biological applications](#)

[Review of Scientific Instruments](#) **78**, 114301 (2007); 10.1063/1.2804771

[Magnetic tweezers for intracellular applications](#)

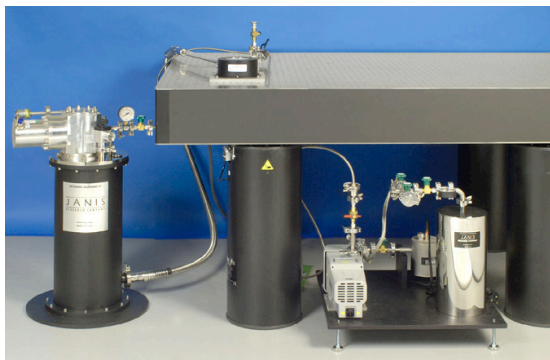
[Review of Scientific Instruments](#) **74**, 4158 (2003); 10.1063/1.1599066

[Magnetic tweezers for DNA micromanipulation](#)

[Review of Scientific Instruments](#) **71**, 4561 (2000); 10.1063/1.1326056

[An optimized software framework for real-time, high-throughput tracking of spherical beads](#)

[Review of Scientific Instruments](#) **85**, 103712 (2014); 10.1063/1.4898178



JANIS

Rising LHe costs? Janis has a solution.
Janis' Recirculating Cryocooler eliminates the use
of Liquid Helium for "wet" cryogenic systems.

sales@janis.com www.janis.com [Click for more information.](#)

Magnetic tweezers optimized to exert high forces over extended distances from the magnet in multicellular systems

L. Selvaggi,^{1,2,a)} L. Pasakarnis,² D. Brunner,² and C. M. Aegerter^{1,2}

¹Department of Physics, University of Zurich UZH, Zurich, Switzerland

²Institute of Molecular Life Science IMLS, Zurich, Switzerland

(Received 26 October 2017; accepted 26 March 2018; published online 11 April 2018)

Magnetic tweezers are mainly divided into two classes depending on the ability of applying torque or forces to the magnetic probe. We focused on the second category and designed a device composed by a single electromagnet equipped with a core having a special asymmetric profile to exert forces as large as 230 pN–2.8 μ m Dynabeads at distances in excess of 100 μ m from the magnetic tip. Compared to existing solutions our magnetic tweezers overcome important limitations, opening new experimental paths for the study of a wide range of materials in a variety of biophysical research settings. We discuss the benefits and drawbacks of different magnet core characteristics, which led us to design the current core profile. To demonstrate the usefulness of our magnetic tweezers, we determined the microrheological properties inside embryos of *Drosophila melanogaster* during the syncytial stage. Measurements in different locations along the dorsal-ventral axis of the embryos showed little variation, with a slight increase in cytoplasm viscosity at the periphery of the embryos. The mean cytoplasm viscosity we obtain by active force exertion inside the embryos is comparable to that determined passively using high-speed video microrheology. *Published by AIP Publishing.*
<https://doi.org/10.1063/1.5010788>

INTRODUCTION

The study of microrheological properties of living organisms is often limited due to the disruptive nature of the correspondingly necessary mechanical manipulation. However, by using minimally invasive methods such as magnetic tweezers (MT), it is possible to locally determine cytoplasmic viscoelasticity inside embryos. Magnetic tweezers apply an external magnetic field to generate a force on superparamagnetic beads. MT are a robust force spectroscopy technique employed in several fields to manipulate single molecules,¹ as magnetic probes inside live cells,² to investigate mechanical properties of biological macromolecules^{3–7} and cancer cells,⁸ to measure biopolymer and single cell microrheology,^{9–12} and to study intracellular applications¹³ and structure-mechanics relationship in biopolymer network,¹⁴ as well as force-regulated processes in developing embryos.^{15–17} The large presence of magnetic tweezers found in the literature demonstrates the usefulness of the method that compared to other powerful techniques, like optical tweezers and atomic force microscopy, presents several advantages. These include no photo-damage, more selectivity in trapping the probe, employment of force as large as hundreds of pN, and the capability of decoupling the imaging from the force paths, which allows the use of any objective lens independently of its numerical aperture. Although MT have become a popular biophysical tool also thanks to their versatility in applying both torques and forces, there are still several limitations in existing solutions. The main drawbacks include the limitation of the time response of the system and the introduction of mechanical noise by moving permanent magnets;¹⁴ the constraint of using at least

two electromagnets to guarantee constant forces over the area of interest;¹³ the constraint in employing long working distance objectives;^{9,17} and the restriction in getting high forces at long distances from the electromagnet,⁹ even producing high power.¹⁷ The necessarily short distance between bead and magnet, imposed by the fact that pN forces can be obtained only close to the magnetic tip, makes present setups incompatible with closed chamber design for live cell imaging and also limit the distance over which the sample can be investigated. Moreover, for bead-core distances of only few micrometers, a sophisticated feedback force control is necessary to ensure an accurate constant force control. The bead movement towards the magnet leads to a steeply increasing force. For bead-core distances of more than 50 μ m, the nonlinearity of the force-distance relationship is instead little pronounced. Motivated by the need to learn more about the microrheology properties of early *Drosophila* embryos to understand how a robust and reproducible syncytial development occurs, we designed MT that overcame the existing limitations and were optimized to exert high constant forces (hundreds of pN) over extended region (>100 μ m) from the magnetic tip to explore unimpeded the entire inside of fly embryos. Although other setups based on permanent magnets^{7,12} exert forces in the same range of our MT, the asset of being able to switch the field and hence the force on and off easily makes our system more useful for the type of investigations we envisage in live embryos. A fly embryo is about 250 μ m in width and 500 μ m in length. Therefore, our MT setup is not limited in applying forces at the periphery of the embryo; rather it is able to exert conspicuous forces also in the middle of the embryo, at a distance of about 120 μ m from the magnetic tip. Magnetic beads have been injected inside embryos and used as probes for the surrounding environment. Viscoelastic properties of the environment of the

^{a)} Author to whom correspondence should be addressed: lara@selvaggi.ch

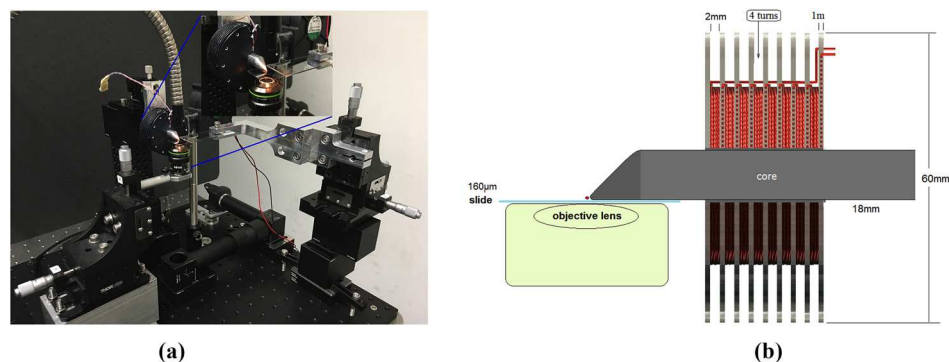


FIG. 1. (a) Picture of the experimental setup. Inset: The magnetic tip sitting on a coverslide used for experiments in fly embryos. (b) Sketch of the magnetic tweezers setup equipped with a single electromagnet used to measure the viscoelastic properties of the cytoplasm of *Drosophila* embryos during early development.

beads have been evaluated from the analysis of the recorded trajectory of the particles.

SETUP DESIGN

Our MT device consists of a single electromagnet, mounted on a homemade inverted microscope, Fig. 1(a), and having the following features:

1. Capability of applying large static constant forces of hundreds of pN on micron-sized beads at distance in excess of 100 μm from the magnetic tip;
2. generation of horizontal forces, exerted perpendicularly to the biological sample;
3. use of any objective lens, from immersion up to long working distance;
4. use of open chambers compatible for live cells imaging;
5. optimization of the cooling system to use coil currents larger than 3 A.

To assure all the listed requirements, we mainly focused on three specifications: coil parameters, cooling system layout, and magnetic core profile.

We performed bright field microscopy by using a small working distance objective (Olympus, 60 \times , 1.42 NA, oil-immersion, PlanApo N) for force calibration and a long working distance objective (Olympus 20 \times) for measurements inside embryos. A 20 \times objective for microrheology investigation inside embryos provides a large field of view (275 $\mu\text{m} \times 206 \mu\text{m}$) that allows controlling the behavior of the overall embryo during the application of the magnetic force. The objective was mounted on a three-axis translational stage to set the relative position between the objective and sample. In order to place one embryo at a time in proximity of the magnetic tip, the position of the sample relative to the magnet was adjusted by a further three-axis micromanipulator. Data were recorded by a CCD camera (Stemmer, IDS UI-3250ML-C-HQ) and acquired at a frame rate of 30 Hz. The velocities and trajectories of the magnetic beads were determined using a tracking plugin in Fiji.

ELECTROMAGNET AND COOLING SYSTEM LAYOUT

The electromagnet employed in our MT device consists of a solenoid with 904 windings of 0.5 mm copper wire wrapped around an aluminum shell. The latter houses an exchangeable

cylindrical core with a tapered tip; see Fig. 1(b). This design allows easy replacement of cores by simply sliding them into the electromagnet. The magnitude of the force produced by the electromagnet (EM) is proportional to the current intensity flowing in the coil up to the saturation of the core material. Our power supply can provide currents ranging from 0.1 to 5 A to the coil. To guarantee reasonably high forces, while minimizing heating of the core, we used a current value of 3.5 A for experiments in *Drosophila* embryos. Using a ferromagnetic core inside the coil, a magnetic flux density gradient of 1100 T/m is achieved in the vicinity of the sample, which then exerts a force of 220 pN on 2.8 μm magnetic beads present inside the embryos. As the coil resistance is 5.3 Ω , we have to dissipate about 65 W. An increase in temperature due to large currents negatively affects the magnetic properties of the core, decreases the amplitude and the gradient of the magnetic field, and transfers heat to the biological sample affecting the experimental results. Therefore, to dissipate heat, we implemented nine 1 mm thick black aluminum fins in the electromagnet design. Fins sprout directly from the aluminum shell, are 1 mm in thickness, and spaced by 2 mm. A fan placed in front of the electromagnet is used to cool down these fins. In this way, each fin is able to dissipate about 5 W, while supplying 3.5 A to the coil. Under these conditions, we measured a temperature increase of 2.5 $^{\circ}\text{C}$ every 15 min next to the magnetic tip. Since the time scale of our experiments was less than a minute, the influence of temperature on the experimental outcome could be neglected.

MAGNETIC CORE PROFILE

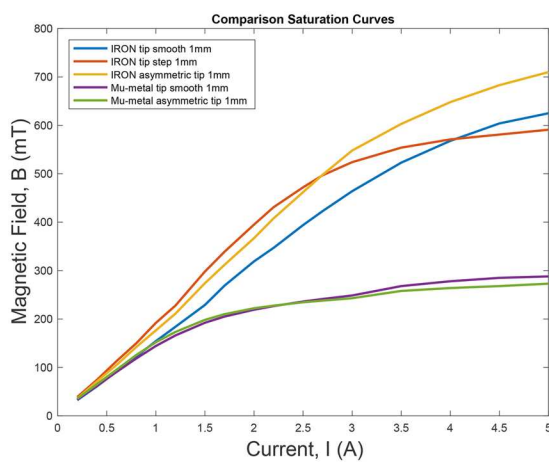
In order to apply forces in the centre of the embryo at a distance larger than 100 μm from the magnetic tip, we compared the magnetic behavior of our tweezers by changing tip length, radius, and shape. For the material of the core, we have chosen ARMCO iron due to its large saturation magnetization. The diameter and length of the core are matched to the coil parameters, i.e., a diameter of 10 mm and a length of 60 mm.

To investigate the applied force in the area of interest, we calculated the field gradient in proximity of the magnetic tip from the measured field distribution for different tip lengths (17 mm and 10 mm) and radii (1 mm and 2 mm). Our experiments are in good agreement with Bijamov simulation results¹⁸ and revealed a significant dependence of the gradient field on the radius of curvature of the tip of the core. This increased

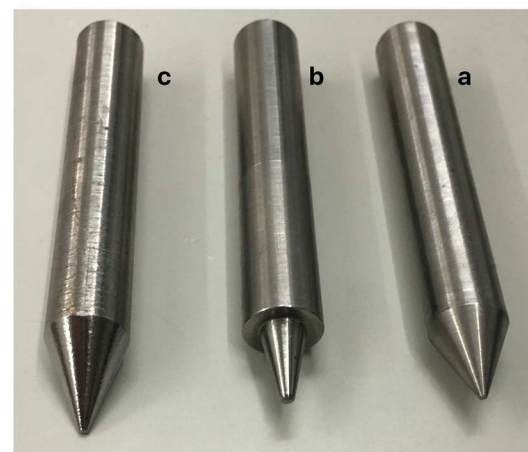
field gradient leads to a threefold increase in force by decreasing the tip radius from 2 mm to 1 mm. On the other hand, the field gradient close to the tip did not change significantly, when the length of the tip is increased (even by a factor of 2).

Finally, we investigated the influence of the overall shape of the tip on the field distribution. We tapered the magnetic core at one end to get three different tip profiles shown in Fig. 2(B): smooth, step, and asymmetric. The tip in the smooth design (a) has a conical shape with a gradually tapered end; the step tip (b) has a conical shape with a step at the initial site of the tip ending in a prominent sharpening. Finally, the asymmetric tip (c), similar to the geometry of the nose of an airplane, was designed to meet the requirements of our experiments. The flat base of the tip is useful to get it near the embryo on the coverslip, while a convergent profile of the top part still guarantees a high magnetic flux gradient in the area of interest. The numerous advantages in using the asymmetric core profile include the following: the possibility to employ a short working distance objective lens, as the latter can be moved unimpeded underneath the glass coverslip, while the magnetic tip lies over the

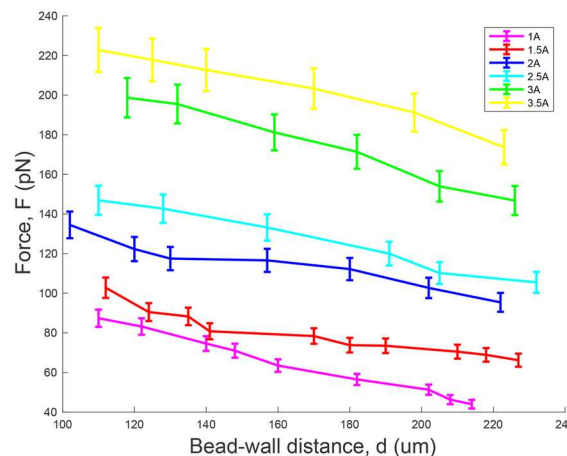
glass next to the embryo; the capability of applying horizontal forces perpendicular to the sample that reveal themselves very convenient for tracking analysis as no other components must be considered; the capability of exerting constant forces by using only a single electromagnet, thanks to both the special asymmetric shape of the tip that allows us to work at long bead-core distances, where the nonlinearity of the force-distance relationship is little pronounced, and the big cross section of the tip (1 mm) that generates a slowly decreasing magnetic field gradient compared to other solutions in which the tip size is usually one hundred times smaller; and therefore to guarantee constant forces, two electromagnets facing each other at 180° must be employed.¹³ Figure 2(A) summarizes the magnetic field magnitude as a function of the current for the different tip profiles. The magnetic field has been measured by putting a Hall probe in contact with the magnetic tip. As can be seen in the picture, differences in tip geometry affect the magnitude of the resulting magnetic field. Our experiments revealed that an iron core with an asymmetric profile and a current of 3.5 A generates a magnetic field of 600 mT. The resulting force at a



(a)



(b)



(c)

FIG. 2. (A) Saturation curves for different core profiles. (B) Suitable profiles for the magnetic tip. From right to left: Smooth (a), step (b), and asymmetric profiles (c). (C) Force calibration curves of $2.8\ \mu\text{m}$ Dynabeads for different current values.

distance of 110 μm from the tip is approximately 230 pN on 2.8 μm superparamagnetic Dynabeads.

FORCE CALIBRATION

A force calibration procedure is required to determine the force as a function of the distance from the magnetic tip. The force magnitude is also a function of the magnetic particle used and the electric current in the coil.¹⁹ To calibrate our magnetic tweezers, we filled a borosilicate glass capillary (square cross section, outer width of 500 μm , and wall thickness of 100 μm) with 2.8 μm Dynabeads diluted in a solution of 70% glycerol in water. In order to delay the onset of fluid flow during calibration, the density of the magnetic beads was kept very low by spacing them at least 10 diameters from each other. In Fig. 2(C), the corresponding measurements of the force calibrations are shown for different currents used for the iron core with the asymmetric profile. Each curve is obtained by tracking the bead location relative to the magnetic tip through a stationary fluid of known viscosity and using viscous friction for a spherical particle $F = 6\pi\eta rv$, where r is the radius of the bead and η is the viscosity of the fluid. By tracking the displacement of a bead subjected to a magnetic force, the velocity versus position dependence can be obtained.

BIOLOGICAL APPLICATIONS

Drosophila melanogaster is a versatile model organism used to study a broad range of phenomena including embryonic development.^{20,21} The early development of *Drosophila* embryos occurs in a syncytium, a single cell containing multiple nuclei that form by 13 division cycles. During the first nine cycles, the nuclei are located in the center of the embryo, while after coordinated nuclear migration the last four cycles mainly take place at its periphery. Subsequently, cellularization separates these peripheral nuclei into individual cells. Syncytial stages are critical for *Drosophila* embryonic patterning and the subsequent cellularization of the embryo. Cytoplasmic properties of the developing syncytium play a critical role by spacing out cellular constituents like nuclei or mitochondria²² and also by modulating the diffusion of key patterning mRNAs and proteins.²³ Knowing the biophysical properties of the syncytium is thus needed to understand how robust, reproducible syncytial development occurs.²⁴

EMBRYO PREPARATION AND INJECTION

The fly strain used in this study was homozygous for sqh:Sqh:GFP, a transgene that encodes GFP fused to the non-muscle myosin II regulatory light chain spaghetti-squash (*sqh*) as described in Ref. 25. Collected embryos were oriented such that they aligned with the anterior-posterior axis parallel to the long axis of the coverslip and with their dorsal side facing the coverslip. The mounted embryos were desiccated at 21 °C in the open for 10-15 min to reduce the inside hydrostatic pressure. This avoids embryo leaking when penetrated with the needle. Embryos were then injected with superparamagnetic beads (Dynabeads M-270, Life Technologies AS,

Norway). These were 2.8 μm in diameter and composed of highly cross-linked polystyrene with 34% magnetic material precipitated in the pores²⁶ To avoid bead aggregation, 1 mg of beads ($\sim 10^9$ beads) was incubated for 15 min with 5 μl Tween-20 diluted in 5 ml of de-ionized water. The beads were then washed with de-ionized water 3 times. For the final injection, beads were re-suspended in 200 μl of de-ionized water.

Injectations were carried out using an upright Zeiss Axiovert X35 microscope equipped with a Narishige MO-11 injection manipulator (Narishige Scientific Instrument Lab, Japan). About 5 min after injection, the glass slide with the injected embryos was placed on a permanent magnet. This pulled the beads closer to the dorsal surface of the embryo, allowing better visualization and confirmation of injection success. In each embryo we often found more than one useful bead for analysis, as after injection beads are spread inside the entire embryo, although only those beads that were spaced at least 10 bead diameters each other were considered for further manipulation.

VISCOSITY IN DIFFERENT REGIONS OF THE EMBRYO

We applied a constant current of 3.5 A to the coil to exert a force of about 220 pN on 2.8 μm beads as obtained from the calibration discussed above. Given the method of injection of particles and the corresponding dilution within the embryo, we did not always observe single beads inside the injected embryos. We often saw clusters of beads. However we excluded these clusters and only single beads were considered for data analysis. This corresponds to a data set of 51 single beads, which were pulled with a constant force inside the embryo at different places as well as inside different embryos. Figure 3 shows a typical field of view and the trace of one single bead pulled inside the embryo. To investigate the heterogeneity of the embryo in greater detail, we used beads injected in three different regions: the center of the embryo, corresponding to a distance range of about 60-140 μm from the magnetic tip, the periphery of the embryo, and center-periphery, which lies between the center and periphery. To exclude any hydrodynamic boundary effects, we defined the periphery of the

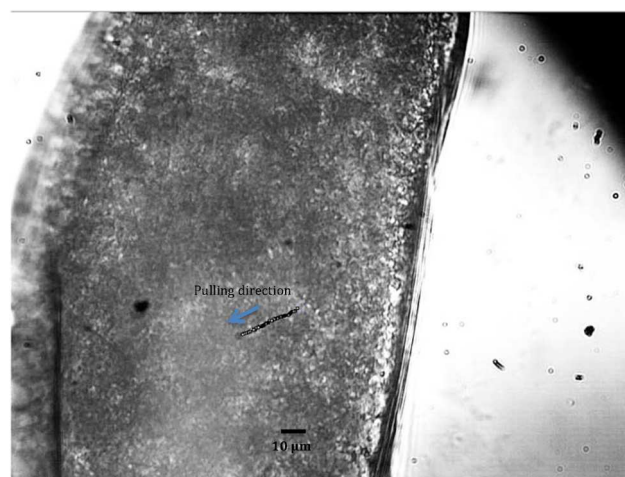


FIG. 3. Trace of a 2.8 μm bead pulled with a constant magnetic force inside a fly embryo. The field of view is 275 $\mu\text{m} \times 206 \mu\text{m}$.

TABLE I: Velocity ranges of single beads injected in different regions along the dorsal-ventral axis of the embryos. Viscosity values in different regions have been calculated by using the Stokes' law.

Velocity ranges	Embryo regions		
	Center	Center-periphery	Periphery
0-5 $\mu\text{m/s}$	14	9	5
5-10 $\mu\text{m/s}$	9	5	4
10-15 $\mu\text{m/s}$	3	1	1
v mean ($\mu\text{m/s}$)^a	5.4 ± 0.7	4.9 ± 0.8	4.8 ± 1.0
η mean (Pa s)^b	0.70 ± 0.1	0.78 ± 0.12	0.79 ± 0.16

^amean velocity of the beads.

^bmean viscosity of the cytoplasm.

embryo as a distance of at least 10 μm from the embryo edge, but no deeper than 30 μm toward the center. Data are reported in Table I. Single beads displayed a mean velocity of $5.4 \pm 0.7 \mu\text{m/s}$ in the center of the embryo, $4.9 \pm 0.8 \mu\text{m/s}$ in the center-periphery region, and $4.8 \pm 1.0 \mu\text{m/s}$ in the periphery. The velocities in the center-periphery regions are similar on either side of the embryo center, while at the periphery next to the magnetic tip they are 15% higher compared to the periphery at the opposite side, due to the distance dependence of the magnetic tweezers. All velocities have been averaged in the above-mentioned results and the errors correspond to standard errors of the mean. Given these velocities of single beads and the corresponding applied force from the calibration curves, we obtain the viscosity of the cytoplasm again by assuming viscous friction acting on the particles inside the cytoplasm. The mean viscosity is found to be $0.70 \pm 0.1 \text{ Pa s}$ in the center region, $0.78 \pm 0.12 \text{ Pa s}$ in the center-periphery region, and $0.79 \pm 0.16 \text{ Pa s}$ in the periphery of the embryo. This means that the interior of the embryo is about three orders of magnitude more viscous than water. Our results are similar to cytoplasm viscosity measured in *Caenorhabditis elegans* embryos²⁷ and *Astropecten aranciacus* starfish oocytes.²⁸ They are also comparable to the measured viscous and elastic moduli of the *Drosophila* embryo cytoplasm using high-speed video microrheology²⁹ and magnetic field.¹⁷ Wessel *et al.* calculated a value of 1.08 Pa for the viscous modulus at intermediate distances (5–40 μm) to the nuclear layer. The slight discrepancy between our results and theirs can be explained by the fact that we used an active technique in which forces were applied differently from the passive tracking approach used by them.

CONCLUSIONS

The aim of this study was twofold: to design magnetic tweezers that were optimized in terms of performance compared to existing devices and at the same time that would allow us to study the microrheological properties within *Drosophila* early embryos. As the overall magnitude of the magnetic field is affected by the size and by the magnetic susceptibility of the magnetic core, while the field distribution depends on the local magnet geometry, we tested different core sizes and profiles to determine our final design. The MT we designed are composed of one single electromagnet equipped with an iron core having a special asymmetric profile. This design leads to several

advantages over existing solutions including the application of large forces over long distances from the magnetic tip, the use of short working distance objective, the possibility to approach the magnetic tip in proximity of the biological sample still applying horizontal forces, and the capability of exerting constant forces by using only a single electromagnet. Our MT are not only specifically adapted for applications in *Drosophila* embryos; indeed the capability of applying hundreds of pN forces to 2.8 μm Dynabeads over distances in excess of 100 μm from the magnetic tip is an interesting feature for many experiments in which the distance-force compromise is a limitation. Our MT experiments consisted of transient magnetic force application to 2.8 μm superparamagnetic beads injected into syncytial blastoderm embryos. Our results showed that the cytoplasm is highly viscous with a viscosity mean value of 0.75 Pa s, where the viscosity increases by about 13% toward the embryo periphery.

ACKNOWLEDGMENTS

We acknowledge Silvio Scherr from the mechanical workshop for the construction and design of dedicated mechanical parts in the setup.

- ¹J. Lipfert, X. Hao, and N. H. Dekker, "Quantitative modeling and optimization of magnetic tweezers," *Biophys. J.* **96**, 5040 (2009).
- ²A. H. B. De Vries, B. E. Krenn, R. van Driel, and J. S. Kanger, "Micro magnetic tweezers for nanomanipulation inside live cells," *Biophys. J.* **88**, 2137 (2005).
- ³C. Gosse and V. Croquette, "Magnetic tweezers: Micromanipulation and force measurement at the molecular level," *Biophys. J.* **82**, 3314 (2002).
- ⁴I. D. Vilfan, J. Lipfert, D. A. Koster, S. G. Lemay, and N. H. Dekker, "Magnetic tweezers for single-molecule experiments," in *Handbook of Single-Molecule Biophysics* (Springer, 2009), p. 371.
- ⁵J. Lipfert, D. A. Koster, I. D. Vilfan, S. Hage, and N. H. Dekker, "Single-molecule magnetic tweezers studies of type IB topoisomerases," *Methods Mol. Biol.* **582**, 71 (2009).
- ⁶D. Kilinc and G. U. Lee, "Advances in magnetic tweezers for single molecule and cell biophysics," *Integr. Biol.* **6**, 27 (2014).
- ⁷H. Chen, H. Fu, X. Zhu, P. Cong, F. Nakamura, and J. Yan, "Improved high-force magnetic tweezers for stretching and refolding of proteins and short DNA," *Biophys. J.* **100**, 517–523 (2011).
- ⁸V. Swaminathan, K. Mythreye, E. T. O'Brien, A. Berchuck, G. C. Globe, and R. Richard Superfine, "Mechanical stiffness grades metastatic potential in patient tumor cells and in cancer cell lines," *Cancer Res.* **71**(15), 5045 (2011).
- ⁹P. Kollmannsberger and B. Fabry, "High-force magnetic tweezers with force feedback for biological applications," *Rev. Sci. Instrum.* **78**, 114301 (2007).
- ¹⁰A. R. Bausch, W. Moller, and E. Sackmann, "Measurement of local viscoelasticity and forces in living cells by magnetic tweezers," *Biophys. J.* **76**, 573 (1999).
- ¹¹B. D. Hoffman and J. C. Crocker, "Cell mechanics: Dissecting the physical responses of cells to force," *Annu. Rev. Biomed. Eng.* **11**, 259 (2009).
- ¹²J. Lin and M. T. Valentine, "High-force NdFeB-based magnetic tweezers device optimized for microrheology experiments," *Rev. Sci. Instrum.* **83**, 053905 (2012).
- ¹³B. G. Hosu, K. Jakab, P. Banki, F. I. Toth, and G. Forgacs, "Magnetic tweezers for intracellular applications," *Rev. Sci. Instrum.* **74**, 4158 (2003).
- ¹⁴Y. Yang, J. Lin, R. Meschewski, E. Watson, and M. T. Valentine, "Portable magnetic tweezers device enables visualization of the three-dimensional microscale deformation of soft biological materials," *Reports* **51**(11), 29 (2011).
- ¹⁵N. Desprat, W. Willy Supatto, P. A. Pouille, E. Beaupaire, and E. Farge, "Tissue deformation modulates twist expression to determine anterior midgut differentiation in *Drosophila* embryos," *Dev. Cell* **15**, 470 (2008).
- ¹⁶G. F. Weber, A. Maureen, M. A. Bjerke, and D. W. A. DeSimone, "Mechanoresponsive Cadherin-Keratin complex directs polarized protrusive behavior and collective cell migration," *Dev. Cell* **17-22**, 104 (2012).

- ¹⁷K. Doubrovinskia, M. Swana, O. Polyakova, and E. F. Wieschaus, "Measurement of cortical elasticity in *Drosophila melanogaster* embryos using ferrofluids," *Proc. Natl. Acad. Sci. U. S. A.* **114**, 1051 (2017).
- ¹⁸A. Bijamov, F. Shubitidze, P. M. Oliver, and D. V. Vezenov, "Quantitative modeling of forces in electromagnetic tweezers," *J. Appl. Phys.* **108**, 104701 (2010).
- ¹⁹M. Tanase, N. Biais, and M. Sheetz, "Magnetic tweezers in cell biology," *Methods Cell Biol.* **83**, 473 (2007).
- ²⁰W. M. Roberts, J. Howard, and A. J. Hudspeth, "Hair cells: Transduction, tuning, and transmission in the inner ear," *Annu. Rev. Cell Biol.* **4**, 63 (1988).
- ²¹E. D. Schejter and E. Wieschaus, "Functional elements of the cytoskeleton in the early *Drosophila* embryo," *Annu. Rev. Cell Biol.* **9**, 67 (1993).
- ²²Y. E. Foe and B. M. Alberts, "Studies of nuclear and cytoplasmic behavior during the five mitotic cycles that precede gastrulation in *Drosophila* embryogenesis," *J. Cell Sci.* **61**, 1 (1983).
- ²³R. Rivera-Pomar and H. Jackle, "From gradients to stripes in *Drosophila* embryogenesis: Filling in the gaps," *Trends Genet.* **12**, 478 (1996).
- ²⁴T. Idema, J. O. Dubuis, L. Kang, M. L. Manning, P. C. Nelson, T. C. Lubensky, and A. J. Liu, "The syncytial *Drosophila* embryo as a mechanically excitable medium," *PLoS One* **8**, e77216 (2013).
- ²⁵A. Royou, C. Field, J. C. Sisson, W. Sullivan, and R. Karess, "Reassessing the role and dynamics of nonmuscle myosin II during furrow formation in early *Drosophila* embryos," *Mol. Biol. Cell* **15**(2), 838 (2004).
- ²⁶G. Fonnuma, C. Johanssonb, A. Molteberga, S. Mørupc, and E. Aksnesa, "Characterisation of Dynabeads® by magnetization measurements and Mössbauer spectroscopy," *J. Magn. Magn. Mater.* **293**, 41 (2005).
- ²⁷B. R. Daniels, B. C. Masi, and D. Wirtz, "Probing single-cell micromechanics *in vivo*: The microrheology of *C. elegans* developing embryos," *Biophys. J.* **90**, 4712 (2006).
- ²⁸G. Pesce, L. Selvaggi, A. Caporali, A. C. De Luca, A. Puppo, G. Rusciano, and A. Sasso, "Mechanical changes of living oocytes at maturation investigated by multiple particle tracking," *Appl. Phys. Lett.* **95**, 093702 (2009).
- ²⁹A. D. Wessel, M. Gumalla, J. Grosshans, and C. F. Schmidt, "The mechanical properties of early *Drosophila* embryos measured by high-speed video microrheology," *Biophys. J.* **108**, 1899 (2015).